Synthesis of Well-Defined Cyclic Poly(*N*-isopropylacrylamide) via Click Chemistry and Its Unique Thermal Phase Transition Behavior

Jian Xu, Jing Ye, and Shiyong Liu*

Department of Polymer Science and Engineering, Joint Laboratory of Polymer Thin Films and Solution, Hefei National Laboratory for Physical Sciences at the Microscale, University of Science and Technology of China, Hefei, Anhui Province 230026, China

Received August 1, 2007; Revised Manuscript Received September 15, 2007

ABSTRACT: We report on the preparation of well-defined cyclic poly(*N*-isopropylacrylamide) (*cyclic*-PNIPAM) via click chemistry and its unique thermal phase transition behavior as compared to the linear counterpart. α-Alkyne-ω-azido heterodifunctional PNIPAM precursor (*linear*-PNIPAM-N_3) was prepared by atom transfer radical polymerization (ATRP) of *N*-isopropylacrylamide in 2-propanol using propargyl 2-chloropropionate as the initiator, followed by reacting with NaN_3 to transform the terminal chloride into azide group. The subsequent end-to-end intramolecular coupling reaction under high dilution and "click" conditions leads to efficient preparation of narrow-disperse *cyclic*-PNIPAM. Gel permeation chromatography (GPC), ^{1}H NMR, Fourier transform infrared (FT-IR), and matrix-assisted laser desorption/ionization time-of-flight (MALDI-TOF) mass spectrometry all confirmed the complete transformation of *linear*-PNIPAM-N_3 to *cyclic*-PNIPAM. The thermal phase transition behavior of *cyclic*-PNIPAM was investigated by temperature-dependent turbidity measurements and micro-differential scanning calorimetry (micro-DSC) and compared to that of *linear*-PNIPAM-N_3 with the same molecular weight. The former possesses lower critical solution temperatures (LCSTs), more prominent concentration dependences of LCST values and cloud points (CPs), broader thermal phase transition range, and prominently lower enthalpy changes (ΔH). The above differences in thermal phase transition behaviors between *cyclic*- and *linear*-PNIPAM should be due to the absence of chain ends and stringent restrictions on backbone conformations in the former.

Introduction

Cyclic polymers have been an intriguing but still less explored topic since their first recognition.[1−4] Because of the absence of chain ends, all repeating units of cyclic polymers are physically and chemically equivalent, and their properties are unaffected by the end groups.[5] In nature, many forms of DNA are cyclic, which can conveniently exclude any possible reactions with terminal groups. Because of the differences in hydrodynamic volumes between linear and cyclic polymers, the latter typically exhibits higher retention time in gel permeation chromatography (GPC) analysis, lower intrinsic viscosity, lower translational friction coefficient, and more rapid decrease of second virial coefficient with molecular weight. In bulk, cyclic polymers possess higher density, molecular weight-dependent melt viscosity, higher refractive index, and higher glass transition temperatures as compared to linear polymers.[6]

Despite the unique properties of cyclic polymers as compared to their linear counterpart, literature reports of cyclic polymers are still rare, probably due to the challenges encountered in their controlled synthesis. Up to date, two main strategies have been developed for the synthesis of cyclic polymers. The first one relies on ring expansion during ring-opening or polycondensation reactions, starting from small building blocks or small molecule monomers.[7−15]

The second strategy is based on the ring-closure reaction of linear polymers under high dilution conditions. Intermolecular coupling reaction occurs between an α,ω-homodifunctional polymer precursor (typically prepared by anionic polymerization) and a complementary bifunctional reactive reagent. Using this principle, cyclic polymers such as polystyrene (PS), poly(2-vinylpyridine) (P2VP), poly(α-methylstyrene), poly(2-vinylnaphthalene), and poly(9,9-dimethyl-2-vinylfluorene) have been successfully prepared by Hogen-Esch and co-workers.[16−19] Tezuka et al.[20] reported highly selective synthesis of cyclic poly(tetrahydrofuran) via the combination of electrostatic self-assembly and subsequent covalent ring closure. Water-soluble cyclic poly(ethylene oxide) (PEO) has been synthesized via reaction with dichloromethane in the presence of solid KOH to attain ring closure via an acetal linkage.[21,22] Nakayama et al.[23] prepared cyclic PEO via UV irradiation of PEO bearing two terminal photodimerizable groups such as cinnamates or coumarinates.

Deffieux and co-workers[24,25] further developed the second strategy through direct unimolecular end-to-end coupling of α,ω-heterodifunctional polymer precursors with two complementary reactive terminal groups. On the basis of similar principles, Kubo et al.[26,27] prepared cyclic PS via intramolecular cyclization of α-carboxyl-ω-amino heterodifunctional linear precursor. Hadjichristidis et al.[28] synthesized a linear α-amino-ω-carboxyl heterodifunctional triblock polymer of styrene, isoprene, and methyl methacrylate, and the subsequent intramolecular cyclization leads to the formation of a cyclic triblock copolymer. However, all of the above examples still suffer from limitations such as low efficiency of cyclization and quite stringent reaction conditions during the preparation of linear precursors. In some cases, the coupling reactions are reversible, and stable covalent linkage cannot be attained.

In the past few years, "click" reactions innovated by Sharpless et al.[29,30] have emerged to be an attractive approach for the formation of stable covalent linkages due to its high efficiency and quantitative yield. Matyjaszewski and co-workers[31] noticed the formation of cyclic side products during the "click" polycondensation reaction of α-alkyne-ω-azido heterodifunctional PS at high concentrations. Grayson et al.[32] later successfully prepared cyclic PS using the heterodifunctional linear PS

* To whom correspondence should be addressed. E-mail: sliu@ustc.edu.cn.

10.1021/ma0717183 CCC: $37.00
Published on Web 11/07/2007

precursor under "click" conditions. Just recently, the "click" approach was employed for the intramolecular ring closure of a single-stranded oligonucleotide.[33]

It should be noted that previous examples of cyclic polymers are mainly hydrophobic, with a few exceptions such as water-soluble cyclic PEO[22] or P2VP.[19] Our recent research interests have focused on stimuli-responsive water-soluble polymers. Poly(*N*-isopropylacrylamide) (PNIPAM) has been the most extensively studied thermoresponsive polymer that exhibits a lower critical solution temperature (LCST) in aqueous solution. Recently, Stöver et al.[34,35] successfully synthesized a series of narrow-disperse PNIPAM with varying molecular weights (MWs) and end groups by atom transfer radical polymerization (ATRP). They found that thermal phase transition temperatures, lower critical solution temperatures (LCSTs) and cloud points (CPs), of PNIPAM homopolymers can vary in the broad range of 32−70 °C depending on their MWs and the hydrophobicity of end groups.

We are quite curious about the thermal phase transition behavior of *cyclic*-PNIPAM. It was quite expected that cyclic conformation of PNIPAM should exhibit some effects on the phase transition as compared to linear ones. Just recently, Lopóz et al.[36] concluded on the basis of Monte Carlo simulations that coil-to-globule transitions of cyclic polymers will occur at lower temperatures (∼2−5% lower) than that of linear polymers with same chain lengths. However, as far as we are aware, experimental confirmation of the above predication still lacks.

In this article, we reported the first example of thermoresponsive water-soluble *cyclic*-PNIPAM via intramolecular "click" cyclization of α-alkyne-ω-azido heterodifunctional PNIPAM linear precursor (*linear*-PNIPAM-N_3), which was prepared by the atom transfer radical polymerization (ATRP) of *N*-isopropylacrylamide (NIPAM) and subsequent nucleophilic substitution reaction with NaN_3. Moreover, we investigated the thermal phase transition behavior of the obtained well-defined and narrow-disperse *cyclic*-PNIPAM via a combination of temperature-dependent turbidity measurements and micro-differential scanning calorimetry (micro-DSC). The obtained results were compared to those of *linear*-PNIPAM with the same MW.

It should be noted that during revision of this manuscript, we noticed a paper just published online by Winnik et al.[37] They synthesized *cyclic*-PNIPAM via a combination of reversible addition-fragmentation chain transfer (RAFT) polymerization and click reaction and reported preliminary results of their phase transition behavior in aqueous solution. The solution properties of *cyclic*-PNIPAM obtained in the current study were then compared to those reported by Winnik et al.[37]

Experimental Section

Materials. *N*-Isopropylacrylamide (97%, Tokyo Kasei Kagyo Co.) was recrystallized twice from benzene/hexane (65:35 v/v) prior to use. Tris(2-aminoethyl)amine (TREN), copper(I) chloride (CuCl, 99.99%), copper(I) bromide (CuBr, 99.99%), propargyl alcohol (99%), and 2,2′-dipyridyl (bpy, 99%) were purchased from Aldrich and used as received. 2-Chloropropionic acid (98%) was purchased from ABCR and used as received. Sodium azide (NaN_3, 99%) was purchased from Alfa Aesar and used without further purification. Tris(2-(dimethylamino)ethyl)amine (Me_6TREN) was synthesized from TREN according to literature procedures.[38] *N*,*N*′-Dicyclohexylcarbodimide (DCC), 4-dimethylaminopyridine (DMAP), 2-propanol, *N*,*N*-dimethylformamide (DMF), and all other chemicals were purchased from Sinopharm Chemical Reagent Co. Ltd. and used as received.

Sample Synthesis. The three-step procedures employed for the preparation of *cyclic*-PNIPAM are shown in Scheme 1.

Scheme 1. Synthetic Routes for the Preparation of Well-Defined Cyclic Poly(*N*-isopropylacrylamide), *cyclic*-PNIPAM, via the Combination of ATRP and Click Reaction

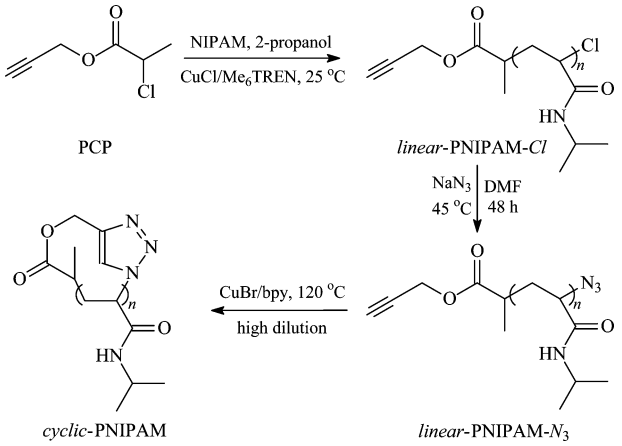

Preparation of Propargyl 2-Chloropropionate (PCP). The ATRP initiator, PCP, was prepared by the esterification reaction of propargyl alcohol with 2-chloropropionic acid in the presence of DCC and DMAP. A typical procedure was as follows. A 250 mL round-bottom flask was charged with 2-chloropropionic acid (10.85 g, 0.10 mol), DCC (22.70 g, 0.11 mol), and methylene chloride (120 mL). The reaction mixture was cooled to 0 °C in an ice−water bath, and a solution of propargyl alcohol (5.61 g, 0.10 mol), DMAP (0.5 g), and methylene chloride (30 mL) was added dropwise over a period of 1 h under magnetic stirring. After the addition was completed, the reaction mixture was stirred at 0 °C for 1 h and then at room temperature for 12 h. After the insoluble *N*,*N*′-dicyclohexylurea was removed by suction filtration, the filtrate was concentrated and then further purified by silica gel column chromatography using methylene chloride as the eluent. After the solvents were removed by rotary evaporator, the obtained residues were distilled under reduced pressure. A colorless liquid was obtained with a yield of ∼84%. ^{1}H NMR ($CDCl_3$, δ, ppm): 4.76 (2H, $-CH_2O-$), 4.43 (H, $-CHCl-$), 2.51 (H, $-C\equiv CH$), and 1.70 (3H, $-CH_3$).

Synthesis of *linear*-PNIPAM-*Cl*.[34,35] The general procedure employed for the preparation of *linear*-PNIPAM-*Cl* was as follows. The mixture containing NIPAM (18.11 g, 160 mmol), Me_6TREN (461 mg, 2 mmol), and 2-propanol (36.22 g) was deoxygenated by bubbling with nitrogen for at least 30 min. CuCl (158 mg, 1.6 mmol) was introduced under the protection of N_2 flow. The reaction mixture was stirred for ∼10 min to allow the formation of CuCl/Me_6TREN complex. PCP (293 mg, 2 mmol) was then added via a microliter syringe to start the polymerization. The reaction was carried out at 25 °C and allowed to stir under nitrogen atmosphere for 3 h. Polymerization was terminated by the addition of a few drops of saturated $CuCl_2$ solution in 2-propanol. The mixture was precipitated into an excess of *n*-hexane. The sediments were collected and redissolved in methylene chloride, and passed through a neutral alumina column using methylene chloride as the eluent to remove copper catalysts. The collected eluents were concentrated and precipitated into an excess of anhydrous diethyl ether. This purification cycle was repeated three times. The obtained product was dried overnight in a vacuum oven for 24 h (overall yield: 55%; $M_{n,GPC} = 8500$, $M_w/M_n = 1.08$).

Synthesis of *linear*-PNIPAM-N_3. In a 100 mL round-bottom flask were added *linear*-PNIPAM-*Cl* (8.5 g), DMF (30 mL), and NaN_3 (325 mg, 5 mmol). The reaction mixture was allowed to stir at 45 °C for 48 h. After most of the DMF was removed at reduced pressure, the remaining portion was diluted with THF, and then precipitated into an excess of anhydrous diethyl ether. The sediments were redissolved in THF, and passed through a neutral alumina column to remove residual sodium salts. The obtained product was dried overnight in a vacuum oven for 24 h (yield: 90%, $M_{n,GPC} = 8600$, $M_w/M_n = 1.08$).

Table 1. Characterization of *linear*- and *cyclic*-Poly(*N*-isopropylacrylamide)

sample code	$M_{n,GPC}$[a]	M_w/M_n[a]	$M_{n,MALDI}$[b]	M_w/M_n[b]	ΔH[c] (kJ/mol)	LCST(°C)[d]	CP(°C)[e]
linear-PNIPAM-*Cl*	8500	1.08				34	37
linear-PNIPAM-N_3	8600	1.08	5950	1.05	5.9	34	37
cyclic-PNIPAM	7500	1.09	6000	1.04	4.2	27	35

[a] Number-average molecular weight, M_n, and polydispersity, M_w/M_n, determined by GPC using DMF as the eluent. [b] Determined by MALDI-TOF mass spectrometry. [c] Enthalpy changes per mole of repeating units associated with thermal phase transition determined by micro-DSC obtained for 2.0 g/L aqueous polymer solutions. [d] Lower critical solution temperature (LCST) was defined as the temperature corresponding to a 1% decrease of transmittance (2.0 g/L). [e] Cloud point (CP) was defined as the temperatures corresponding to a 50% decrease of transmittance (2.0 g/L).

Synthesis of *cyclic*-PNIPAM. To a 2.5 L three-necked round-bottom flask was added 1.0 L of DMF, and then it was thoroughly deoxygenated by bubbling with nitrogen for ~2 h. CuBr (143 mg, 1 mmol) and bpy (312 mg, 2 mmol) were introduced into the flask under protection of N_2 flow. A separate 100 mL round-bottom flask containing 0.2 g of *linear*-PNIPAM-N_3 dissolved in 20 mL of DMF was degassed via two freeze/pump/thaw cycles. Under vigorous magnetic stirring and the protection of N_2 flow, this solution was slowly added into the 2.5 L flask (thermostated at 120 °C) via a microliter syringe at a rate of 100 μL/10 min. After the addition was completed, the reaction mixture was allowed to stir for 2 h at 120 °C. After the mixture was cooled to ~40 °C, DMF was removed under reduced pressure, and the flask was thoroughly washed with methylene chloride. The combined washings were concentrated and then precipitated to an excess of anhydrous diethyl ether. After redissolving in methylene chloride, the product was further purified by passing through a neutral alumina column to remove the copper catalysts and by precipitation into anhydrous ethyl ether. The obtained product was dried overnight in a vacuum oven for 24 h (yield: 60%, $M_{n,GPC} = 7500$, $M_w/M_n = 1.09$).

Step-Growth Click Coupling of *linear*-PNIPAM-N_3. *linear*-PNIPAM-N_3 (0.5 g), CuBr (14 mg, 0.1 mmol), bpy (31 mg, 0.2 mmol), and DMF (2 mL) were added into a 10 mL glass ampule. The mixture was subjected to two freeze/pump/thaw cycles and then flame-sealed under vacuum. The reaction mixture was allowed to stir at ambient temperature for 12 h. After precipitation into an excess of anhydrous diethyl ether, the sediments were dissolved in THF, passed through a neutral alumina column, and reprecipitated into diethyl ether. The product was dried in a vacuum oven overnight at room temperature for 12 h (yield: 95%).

Characterization. Molecular weights and molecular weight distributions were determined by gel permeation chromatography (GPC) using a series of three linear Styragel columns (HT2, HT4, and HT5) and an oven temperature of 50 °C. A Waters 1515 pump and Waters 2414 differential refractive index detector (set at 30 °C) were used. The eluent was DMF at a flow rate of 1.0 mL/min. All ^{1}H NMR spectra were recorded in $CDCl_3$ using a Bruker 300 MHz spectrometer. Fourier transform infrared (FT-IR) spectra were recorded on a Bruker VECTOR-22 IR spectrometer. The spectra were collected over 64 scans with a spectral resolution of 4 cm^{-1}.

Matrix-Assisted Laser Desorption/Ionization Time-of-Flight (MALDI-TOF) Mass Spectrometry. The MALDI-TOF mass spectrum was recorded in the reflector mode on a Bruker BIFLEXe III mass spectrometer using a nitrogen laser (337 nm) and an accelerating potential of 20 kV. 2,5-Dihydroxybenzoic acid (DHB) (99%, Sigma) was used as the matrix, and $NaBF_4$ was added to improve the ionization.

Temperature-Dependent Turbidimetry. The optical transmittance of the aqueous solution of *linear*- or *cyclic*-PNIPAM at a wavelength of 500 nm was acquired on a Unico UV/vis 2802PCS spectrophotometer. A thermostatically controlled cuvette was employed, and the heating rate was 0.2 °C min^{-1}. The lower critical solution temperature (LCST) and the cloud point (CP) were defined as the temperatures corresponding to 1% and 50% decreases of transmittance, respectively.

Micro-Differential Scanning Calorimetry (micro-DSC) Characterization. Micro-DSC measurements were carried out on a VP DSC from MicroCal. The volume of the sample cell was 0.509 mL. The reference cell was filled with deionized water. The sample solution with a concentration of 2.0 g/L was degassed at 25 °C for half an hour and equilibrated at 10 °C for 2 h before the heating process with the heating rate of 1.0 °C/min.

Results and Discussion

As shown in Scheme 1, the synthesis of *cyclic*-PNIPAM was achieved in three steps. It proceeded first with the preparation of α-alkyne-ω-chloro heterodifunctional PNIPAM, *linear*-PNIPAM-*Cl*, by ATRP, followed by its transformation to α-alkyne-ω-azido heterodifunctional PNIPAM, *linear*-PNIPAM-N_3, via nucleophilic substitution reaction with NaN_3, and the subsequent intramolecular "click" ring closure under high dilution conditions. The structural parameters of *linear*- and *cyclic*-PNIPAM samples are summarized in Table 1.

Preparation of *linear*-PNIPAM Precursors. Polymer samples produced by ATRP under "controlled" conditions can well-preserve the terminal halogen atom, which can be successfully converted into azide group. Thus, the combination of ATRP and click reaction has been proved to be a highly efficient and convenient approach for the preparation of polymers with complex structures.[39−41] At the beginning of ATRP history, acrylamido monomers were considered difficult to polymerize in a controlled manner. On the basis of progresses obtained by research groups of Matyjaszewski,[42,43] Brittain,[44] and Masci et al.,[45] Stöver and his co-workers[34,35] successfully synthesized PNIPAM with low polydispersity in various alcohols by using methyl 2-chloropropionate as the initiator and CuCl/Me_6TREN as the catalysts.

In the current study, similar protocols were employed for the ATRP of NIPAM monomer. *linear*-PNIPAM-*Cl* was prepared using the PCP/CuCl/Me_6TREN system at 25 °C in 2-propanol. Grayson et al.[32] successfully prepared α-alkyne-ω-chloro heterodifunctional PS by ATRP using propargyl 2-bromoisobutyrate as the initiator, indicating that the terminal alkyne moiety does not interfere with the polymerization and the trimethylsilyl protection chemistry is unnecessary. The NIPAM polymerization was terminated at relatively low monomer conversions (~65%) with $CuCl_2$, ensuring a high degree of terminal chlorine functionality.

The DMF GPC trace of *linear*-PNIPAM-*Cl* precursor was shown in Figure 1, revealing a relatively sharp and symmetric peak. No tailing or shoulder at the lower or higher molecule weight side could be discerned, indicating the absence of premature chain termination, which agrees quite well with the results obtained by Stöver et al.[34,35] GPC analysis of *linear*-PNIPAM-*Cl* in DMF resulted in a number-average molecular weight, $M_{n,GPC}$, of 8500 and a polydispersity, M_w/M_n, of 1.08. Subsequently, the terminal chlorine was transformed into azide group by simple nucleophilic substitution reactions in DMF in the presence of an excess of NaN_3. After purification, GPC results indicated that the elution peak of *linear*-PNIPAM-N_3 remains basically the same as that of *linear*-PNIPAM-*Cl*, revealing an $M_{n,GPC}$ of 8600 and an M_w/M_n of 1.08 (Table 1).

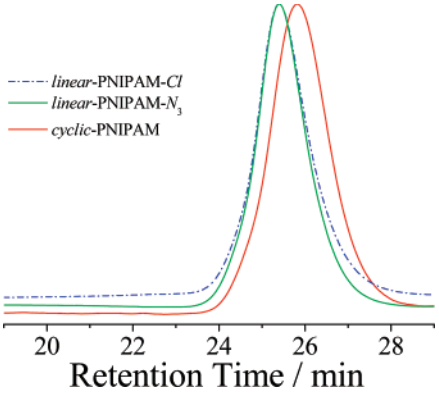

Figure 1. GPC traces obtained for *linear*-PNIPAM-*Cl* and *linear*-PNIPAM-N_3 precursors, and *cyclic*-PNIPAM synthesized via intramolecular click reaction in DMF under high dilution conditions.

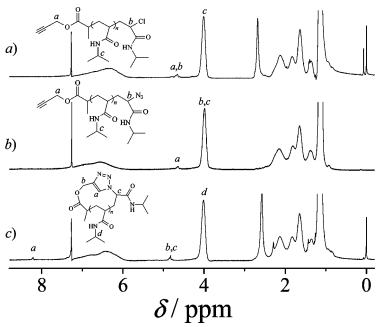

Figure 2. ^{1}H NMR spectra of (a) *linear*-PNIPAM-*Cl*, (b) *linear*-PNIPAM-N_3, and (c) *cyclic*-PNIPAM in $CDCl_3$.

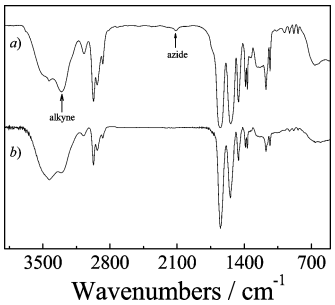

Figure 3. FT-IR spectra obtained for (a) *linear*-PNIPAM-N_3 and (b) *cyclic*-PNIPAM.

^{1}H NMR spectra and the corresponding peak assignments of *linear*-PNIPAM-*Cl* and *linear*-PNIPAM-N_3 are shown in Figure 2. For *linear*-PNIPAM-*Cl*, peaks a and b overlapping at ~4.6 ppm can be ascribed to methylene protons (2H) of propargyl residues and methine proton (1H) neighboring to terminal chlorine (Figure 2a). After *linear*-PNIPAM-*Cl* reacted with NaN_3, resonance signals of methylene protons (2H) of propargyl residue still locate at 4.6 ppm, whereas that of methine proton (1H) neighboring to azido group shifts to ~4.0 ppm. Using peak c characteristic of methine proton of NIPAM repeating units as a reference, integral ratio of resonance peaks at 4.6 ppm with that at 4.0 ppm in Figure 2b (*linear*-PNIPAM-N_3) decreases about 30%, as compared to that calculated from Figure 2a (*linear*-PNIPAM-*Cl*). This strongly suggests complete transformation of terminal chlorine into azido groups. Moreover, the FT-IR spectrum of *linear*-PNIPAM-N_3 clearly revealed the appearance of a new absorbance peak at ~2110 cm^{-1}, which is characteristic of the terminal azido group (Figure 3).

Intramolecular "Click" Cyclization. The intramolecular cyclization reaction was achieved under high dilution conditions by the end-to-end "click" reaction between terminal alkyne and azide groups on *linear*-PNIPAM-N_3 precursor (Scheme 1). Quite stringent "click" reaction conditions (120 °C, DMF, CuBr/bpy) were employed to ensure the fast and complete ring closure of previously added *linear*-PNIPAM-N_3 before the next addition, thanks to the high efficiency and quantitative yield of click reactions under the current conditions. A rough calculation indicated that the highest weight concentration of *linear*-PNIPAM-N_3 in DMF during the ring-closure reaction was ~1×10^{-6} g/mL.

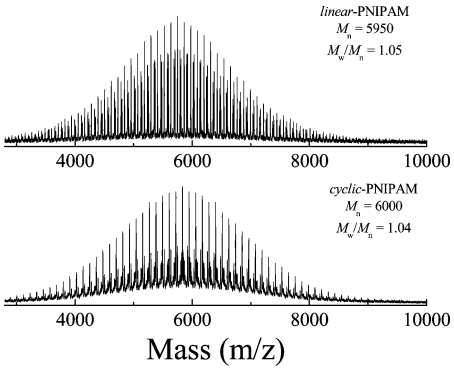

Figure 4. MALDI-TOF mass spectra of *linear*-PNIPAM-N_3 precursor and *cyclic*-PNIPAM.

GPC analysis of the obtained *cyclic*-PNIPAM in DMF resulted in an $M_{n,GPC}$ of 7500 and an M_w/M_n of 1.09 (Figure 1, Table 1). Most importantly, we can also clearly observe a clean shift of the elution peak of *cyclic*-PNIPAM to the lower molecular weight side, as compared to that of *linear*-PNIPAM-N_3 precursor. In the 1940s, Kramers et al.[1] and Zimm et al.[2] theoretically predicted that the average radius of gyration, $\langle R_g \rangle$, of a random coil linear polymer to that of a cyclic polymer should be 2.0, which was later experimentally confirmed by neutron scattering in 1979.[4] Thus, the shift to lower molecular weight side for *cyclic*-PNIPAM can be clearly ascribed to its much lower hydrodynamic volume as compared to that of *linear*-PNIPAM-N_3.

It is worthy of noting that GPC traces of both *linear*-PNIPAM and *cyclic*-PNIPAM are monomodal and symmetric, revealing the absence of peaks or shoulders at the higher molecular weight side. This strongly suggests that intermolecular condensation does not occur under the current high dilution conditions.

Figure 2c shows the ^{1}H NMR spectrum of *cyclic*-PNIPAM; we can observe the appearance of a new resonance peak at 8.2 ppm after "click" cyclization, which can be ascribed to the proton of triazole ring. As compared to that of *linear*-PNIPAM-N_3, peaks a and b initially at 4.6 and 4.0 ppm (Figure 2b) completely shifted to ~4.8 ppm (Figure 2c). Thus, ^{1}H NMR results suggested successful ring closure of *linear*-PNIPAM-N_3 via the "click" mechanism.

The intramolecular end-to-end "click" cyclization reaction was further confirmed by FT-IR spectroscopy and MALDI-TOF mass spectrometry. From Figure 3, we can observe the complete disappearance of characteristic azide absorbance peak at ~2110 cm^{-1} for *cyclic*-PNIPAM, as compared to that of *linear*-PNIPAM. Moreover, the relative intensity of the absorbance peak at 3310 cm^{-1} characteristic of terminal alkyne groups also decreased considerably. This further confirmed that the intramolecular "click" ring closure was almost complete.

The MALDI-TOF mass spectra of *linear*-PNIPAM-N_3 and *cyclic*-PNIPAM samples are shown in Figure 4. 2,5-Dihydroxybenzoic acid was used as the matrix, and $NaBF_4$ was added to improve the ionization, resulting in the formation of M/Na^+. Figure 4 shows two envelope of peaks centered at ~5800 Da,

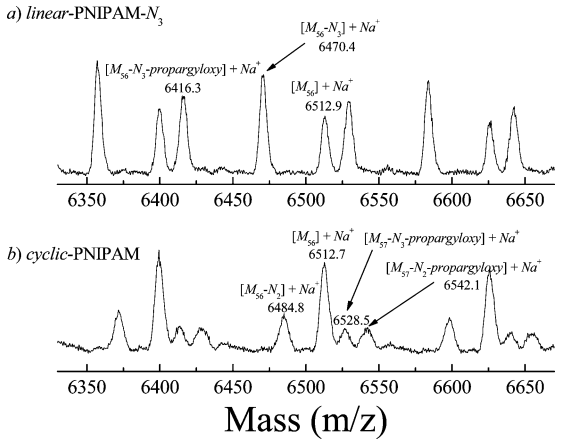

Figure 5. Expanded MALDI-TOF mass spectra in the mass range of 6330−6670 Da obtained for (a) *linear*-PNIPAM-N_3 and (b) *cyclic*-PNIPAM, respectively.

extending from 3000 to 8500 Da. These MALDI data give $M_{n,MALDI}$ of 5950 and M_w/M_n of 1.05 for *linear*-PNIPAM-N_3 and $M_{n,MALDI}$ of 6000 and M_w/M_n of 1.04 for *cyclic*-PNIPAM (Table 1). The MALDI-TOF data can further verify that the molecular weights of *linear*- and *cyclic*-PNIPAM are almost the same before and after intramolecular "click" cyclization. It should also be noted that there exist no peaks at the higher molecular weight side in the mass spectrum of *cyclic*-PNIPAM, confirming again that intermolecular coupling or condensation does not occur and the "click" reaction is presumably intramolecular.

Detailed descriptions of the MALDI-TOF mass spectra were given in Figure 5. The expanded spectrum of *linear*-PNIPAM-N_3 reveals a repeating set of three peaks separated from neighboring sets by 113.2 Da corresponding to the molar mass of NIPAM unit. The three peaks are ascribed to chains bearing different chain ends. For instance, the peaks at *m*/*z* values of 6512.9, 6470.4, and 6416.3 Da can be ascribed to $(NIPAM)_{56}/Na^+$ (6508.8 calcd), $(NIPAM)_{56}$-N_3/Na^+ (6466.7 calcd), and $(NIPAM)_{56}$-N_3-propargyloxy/Na^+ (6411.7 calcd), respectively. On the other hand, the expanded spectrum of *cyclic*-PNIPAM reveals a repeating set of four peaks separated from neighboring sets by 113.2 Da, and the peaks at *m*/*z* values of 6484.8, 6512.7, 6528.5, and 6542.1 Da correspond to $(NIPAM)_{56}$-N_2/Na^+ (6480.7 calcd), $(NIPAM)_{56}/Na^+$ (6508.8 calcd), $(NIPAM)_{57}$-N_3-propargyloxy/Na^+ (6524.8 calcd), and $(NIPAM)_{57}$-N_2-propargyloxy/Na^+ (6538.8 calcd), respectively. The above peak assignments for *linear*- and *cyclic*-PNIPAM suggested that the former possesses a high degree of end functionality and the latter has been obtained with quite high purity.

Step-Growth Click Coupling of *linear*-PNIPAM-N_3. To further check the degree of end functionality of *linear*-PNIPAM-N_3 precursor and the possibility of intermolecular condensation reaction, the "click" reaction was also conducted at high concentration (25.0 wt/v %) to facilitate the coupling reaction of α-alkyne-ω-azido heterodifunctional PNIPAM linear precursor. As compared to that of *linear*-PNIPAM-N_3 showing a peak molecular weight, M_p, of 8700, the intermolecular coupling product (*coupling*-PNIPAM) exhibits a bimodal elution peak, with M_p values being 706 600 and 18 300, respectively (Figure 6). The higher molecular weight peak can be clearly ascribed to the intermolecular condensation product, consisting of ∼81 sequences of the linear precursor.

For the main peak with an M_p of 18 300, we tentatively ascribe it to dimer product resulting from "click" condensation of two linear precursors. For PNIPAM chains with molecular

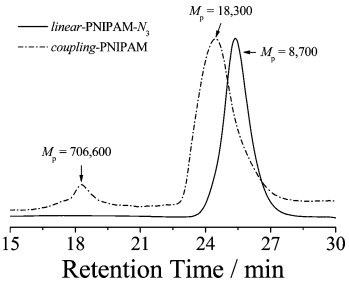

Figure 6. GPC traces obtained for *linear*-PNIPAM-N_3 precursor and intermolecular coupling product (*coupling*-PNIPAM) via click reaction at a concentration of 25 wt/v % in DMF.

weights (MW) of 6000 and 12 000, the end group mobility might differ considerably. PNIPAM chains with a MW of 12 000 should take a more "coiled" conformation, burying terminal azido and alkynyl groups within coils and restricting intermolecular condensation reactions. It should be noted that for "click" polycondensation products of α-alkyne-ω-azido heterodifunctional PS at high concentrations as reported by Matyjaszewski et al.,[31] we can also discern the formation of dimers.

On the basis of basic theories of polycondensation reactions,[46] we can at least conclude that the degree of end functionality of *linear*-PNIPAM-N_3 should be quite high; otherwise, we would not observe the formation of high molecular weight product.

Thermal Phase Transition Behavior of *cyclic*-PNIPAM and *linear*-PNIPAM-N_3. Thermal phase transition temperature, expressed as lower critical solutions temperature (LCST) and/or cloud point (CP), is one of the basic physical properties of thermoresponsive water-soluble polymers. For linear PNIPAM homopolymers, Stöver et al.[35] recently elucidated the effects of end group hydrophobicity and molecular weight on their CP values. In the current case, *linear*-PNIPAM-N_3 and *cyclic*-PNIPAM possess the same molecular weight (Figures 4 and 5), but the latter possesses no chain ends. Thus, they prove to be a suitable system for the investigation of chain topology effects on the thermal phase transition behavior of PNIPAM.

Temperature-dependent turbidimetry was then employed to determine LCST and CP values of *linear*-PNIPAM-N_3 and *cyclic*-PNIPAM in aqueous solutions. It should be noted that CP is a macroscopic parameter defining the temperature at which the solution turns turbid, which can also be checked by visual inspection. On the other hand, LCST is a thermodynamic parameter defining the critical temperature at which interchain aggregation starts to occur. For convenience and direct comparison to the results obtained by Winnik et al.,[37] in subsequent sections, LCST and CP values were defined as the temperature at which 1% and 50% decreases of transmittance could be observed, respectively.

Figure 7a shows temperature-dependent transmittance at a wavelength of 500 nm obtained for aqueous solutions of *cyclic*-PNIPAM and *linear*-PNIPAM-N_3 at a polymer concentration of 2.0 g/L. We can clearly see that, above 27 and 34 °C, transmittance starts to decrease for *cyclic*-PNIPAM and *linear*-PNIPAM-N_3, respectively. This indicates that, above these two critical temperatures, interchain aggregation starts to occur, and scattering of the incident light due to the presence of aggregates will tend to decrease optical transmittance. Thus, LCST values of *cyclic*-PNIPAM and *linear*-PNIPAM-N_3 have been determined to be 27 and 34 °C, respectively (Figure 7a). It is well known that PNIPAM with decreasing MW possesses higher LCST;[35] thus, for *linear*-PNIPAM-N_3 with an MW of 6000, the LCST value of 34 °C is quite reasonable as compared to that typically reported for linear PNIPAM (MW > 10^4,

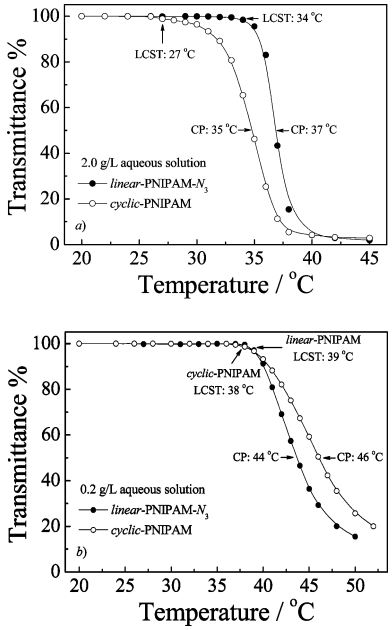

Figure 7. Temperature dependences of optical transmittance at 500 nm obtained for (a) 2.0 g/L and (b) 0.2 g/L aqueous solutions of *linear*-PNIPAM-N_3 and *cyclic*-PNIPAM. The lower critical solution temperature (LCST) and the cloud point (CP) were defined as the temperatures corresponding to 1% and 50% decreases of transmittance, respectively.

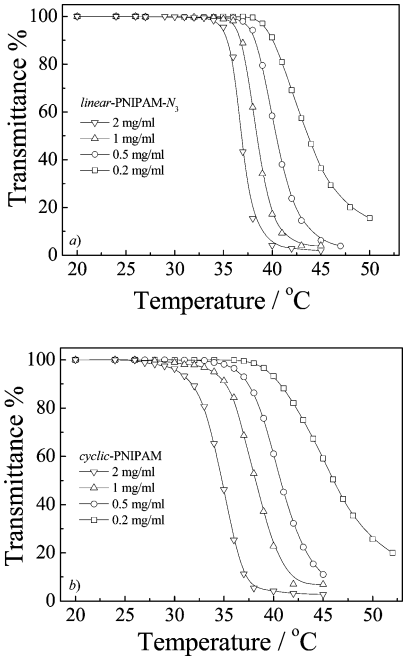

Figure 8. Temperature dependences of optical transmittance at 500 nm obtained for aqueous solutions of (a) *linear*-PNIPAM-N_3 and (b) *cyclic*-PNIPAM at varying polymer concentrations.

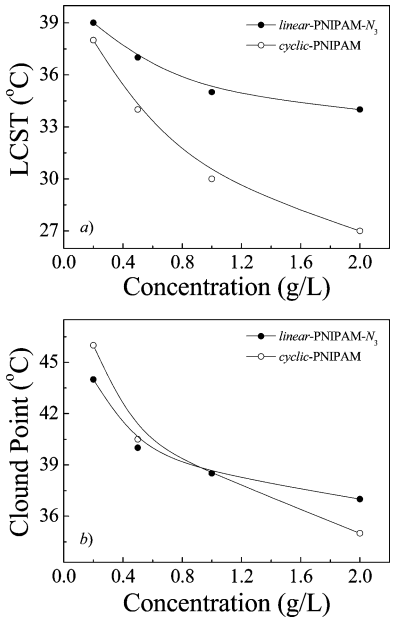

Figure 9. Concentration dependences of (a) LCSTs and (b) CPs obtained for aqueous solutions of *linear*-PNIPAM-N_3 and *cyclic*-PNIPAM, respectively. LCST and CP values were defined as the temperatures corresponding to 1% and 50% decreases of transmittance, respectively.

~32 °C). On the other hand, the obtained LCST value (27 °C) for *cyclic*-PNIPAM (MW ≈ 6000, 2.0 g/L) is unprecedented; this must be due to the ring structure taken by *cyclic*-PNIPAM and the absence of any chain ends. This is in general agreement with that proposed by López et al.[36] based on Monte Carlo simulations.

At a polymer concentration of 2.0 g/L, we can also observe from Figure 7a that *linear*-PNIPAM-N_3 exhibits a relatively sharp decrease of transmittance, whereas *cyclic*-PNIPAM shows a more gradual decrease of transmittance, spanning a temperature range of ~13 °C. The CP values (50% transmittance decrease) of *cyclic*-PNIPAM and *linear*-PNIPAM-N_3 are determined to be 35 and 37 °C, respectively. Table 1 summarizes CP and LCST values obtained for *cyclic*-PNIPAM and *linear*-PNIPAM-N_3 at a concentration of 2.0 g/L.

Figure 7b shows the temperature-dependent transmittance at a much lower polymer concentration (0.2 g/L). The obtained CP values of *cyclic*-PNIPAM and *linear*-PNIPAM-N_3 are 46 and 44 °C, respectively. Thus, the relative magnitude of CP values of *cyclic*-PNIPAM and *linear*-PNIPAM-N_3 strongly depends upon polymer concentrations. Figure 8 shows the temperature-dependent transmittance obtained for aqueous solutions of *linear*-PNIPAM-N_3 and *cyclic*-PNIPAM at different concentrations. In both cases, we can clearly see that both LCST and CP values increase with decreasing polymer concentrations and that the lower is the polymer concentration, the broader is the temperature range exhibiting the decrease of transmittance.

Figure 9 illustrates the effects of polymer concentrations on LCST and CP values for *linear*-PNIPAM-N_3 and *cyclic*-PNIPAM samples. As the polymer concentrations decrease from 2.0 to 0.2 g/L, LCST values increase from 34 to 39 °C for *linear*-PNIPAM-N_3, and from 27 to 38 °C for *cyclic*-PNIPAM (Figure 9a). On the other hand, upon decreasing the polymer concentrations from 2.0 to 0.2 g/L, CP values increase from 37 to 44 °C for *linear*-PNIPAM-N_3, and from 35 to 46 °C for *cyclic*-PNIPAM (Figure 9b).

It is worthy of noting that in the polymer concentration range of 0.2−2.0 g/L, LCST values of *cyclic*-PNIPAM are systematically lower than those obtained for the linear counterpart (Figure 9a). On the other hand, CP values of *cyclic*-PNIPAM are larger than those of *linear*-PNIPAM-N_3 at lower polymer concentrations, but smaller at higher polymer concentrations (Figure 9b).

The current definition of CP (50% transmittance decrease) will not be applicable for PNIPAM solutions with extremely low concentrations, as the optical transmittance might not decrease to the extent of 50%. Under similar conditions, LCST values can still be safely obtained from temperature-dependent optical transmittance or scattered light intensity curves.

From Figure 9, we can also tell that the *cyclic*-PNIPAM exhibits more prominent concentration dependences of CP and

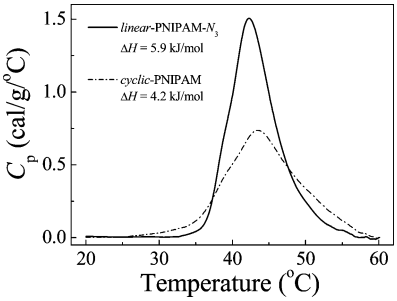

Figure 10. Temperature dependence of the specific heat capacity (C_p) obtained for 2.0 g/L aqueous solutions of *linear*-PNIPAM-N_3 and *cyclic*-PNIPAM during the heating process. The heating rate was 1.0 °C/min.

LCST values as compared to that of *linear*-PNIPAM. In the paper recently published by Winnik et al.,[37] they reported CP values (50% transmittance decrease) of 37 and 44 °C for *linear*-PNIPAM and *cyclic*-PNIPAM with an MW of 6000 at a polymer concentration of 1.0 g/L. In our case, we obtain a CP value of ~38 °C at a polymer concentration of 1.0 g/L for both *linear*-PNIPAM and *cyclic*-PNIPAM with comparable MW (6000) (Figure 9b). We are currently unclear about the discrepancy of CP values reported by us and those by Winnik et al.[37]

Micro-DSC was further employed to investigate the thermal phase transitions of *linear*- and *cyclic*-PNIPAM samples in aqueous solution at a concentration of 2.0 g/L, and the results are shown in Figure 10. Apparently, the endothermic peak of *cyclic*-PNIPAM is much broader than that of *linear*-PNIPAM-N_3. Moreover, the onset temperatures of C_p increase are ~26 and 33 °C for *cyclic*-PNIPAM and *linear*-PNIPAM-N_3, respectively. These critical temperatures are in good agreement with the LCST values determined by temperature-dependent turbidimetry (Figures 7−9).

It has been well-established that the enthalpy changes (ΔH) associated with the thermal phase transition of linear PNIPAM homopolymer are in the range of 5.5−7.5 kJ per mole of repeating units.[47−49] Micro-DSC endothermic peaks shown in Figure 10 allow the calculation of ΔH, which are 5.9 and 4.2 kJ/mol for *linear*-PNIPAM-N_3 and *cyclic*-PNIPAM polymers, respectively (Table 1). It should be noted that ΔH values obtained for *linear*-PNIPAM-N_3 and *cyclic*-PNIPAM are quite comparable to those reported by Winnik et al.[37]

The obtained ΔH for *linear*-PNIPAM-N_3 basically falls in the reported ΔH range. The much lower (~30%) ΔH value of *cyclic*-PNIPAM as compared to that of *linear*-PNIPAM-N_3 is unprecedented and quite intriguing. It is worthy of noting that the ΔH value is closely associated with the energy required for the breakup of ca. one hydrogen bond pair between one repeating unit and water molecules upon phase transitions. Considering that hydrogen-bonding interactions possess high directionality and that the cyclic topology will exert stringent restrictions on backbone conformation for *cyclic*-PNIPAM, the lower ΔH value of *cyclic*-PNIPAM as compared to that of *linear*-PNIPAM-N_3 must be due to the reduced number of hydrogen-bonding interaction pairs and/or weakened hydrogen-bonding interactions. In an alternate explanation, *linear*-PNIPAM-N_3 chains are random coils in aqueous solution, and they will expose more accessible surface areas to water than *cyclic*-PNIPAM chains, which typically possess more compact conformations. This will also lead to the changes of number and/or strength of hydrogen-bonding interactions between water molecules and NIPAM repeating units.

Conclusion

We successfully demonstrate that thermoresponsive water-soluble *cyclic*-PNIPAM with narrow polydispersity can be successfully synthesized via intramolecular end-to-end "click" cyclization of α-alkyne-ω-azido heterodifunctional PNIPAM linear precursor under high dilution conditions. Possessing no chain ends, *cyclic*-PNIPAM exhibits unique thermal phase transition behavior, which is drastically different from that of *linear*-PNIPAM-N_3 with the same molecular weight. The cyclic topology exerts stringent restrictions on backbone conformation for *cyclic*-PNIPAM, leading to its lower LCST values, stronger concentration dependences of LCST and CP values, and smaller ΔH value associated with thermal phase transitions, as compared to *linear*-PNIPAM. As far as we are aware, these intriguing results obtained for the thermal phase transitions of thermoresponsive cyclic polymers are intriguing and worthy of further theoretical considerations.

Acknowledgment. This work was financially supported by an Outstanding Youth Fund (50425310) and research grants (20534020 and 20674079) from the National Natural Scientific Foundation of China (NNSFC), the "Bai Ren" Project and Special Grant (KJCX2-SW-H14) of the Chinese Academy of Sciences, and the Program for Changjiang Scholars and Innovative Research Team in University (PCSIRT).

References and Notes

(1) Kramers, H. A. *J. Chem. Phys.* **1946**, *14*, 415−424.
(2) Zimm, B. H.; Stockmayer, W. H. *J. Chem. Phys.* **1949**, *17*, 1301−1314.
(3) Casassar, E. F. *J. Polym. Sci.* **1964**, *3*, 605−614.
(4) Higgins, J. S.; Dodgson, K.; Semlyen, J. A. *Polymer* **1979**, *20*, 553−558.
(5) McLeish, T. *Science* **2002**, *297*, 2005−2006.
(6) Semlyen, J. A. *Cyclic Polymers*, 2nd ed.; Kluwer Academic Publishers: Boston, 2000.
(7) Bielawski, C. W.; Benitez, D.; Grubbs, R. H. *Science* **2002**, *297*, 2041−2044.
(8) He, T.; Zheng, G. H.; Pan, C. Y. *Macromolecules* **2003**, *36*, 5960−5966.
(9) Takeuchi, D.; Inoue, A.; Osakada, K.; Kobayashi, M.; Yamaguchi, K. *Organometallics* **2006**, *25*, 4062−4064.
(10) Endo, K.; Yamanaka, T. *Macromolecules* **2006**, *39*, 4038−4043.
(11) Kricheldorf, H. R.; Fritsch, D.; Vakhtangishvili, L.; Lomadze, N.; Schwarz, G. *Macromolecules* **2006**, *39*, 4990−4998.
(12) van Dijk, M.; Mustafa, K.; Dechesne, A. C.; van Nostrum, C. F.; Hennink, W. E.; Rijkers, D. T. S.; Liskamp, R. M. J. *Biomacromolecules* **2007**, *8*, 327−330.
(13) Li, H. Y.; Debuigne, A.; Jerome, R.; Lecomte, P. *Angew. Chem., Int. Ed.* **2006**, *45*, 2264−2267.
(14) Culkin, D. A.; Jeong, W. H.; Csihony, S.; Gomez, E. D.; Balsara, N. R.; Hedrick, J. L.; Waymouth, R. M. *Angew. Chem., Int. Ed.* **2007**, *46*, 2627−2630.
(15) Chisholm, M. H.; Gallucci, J. C.; Yin, H. F. *Proc. Natl. Acad. Sci. U.S.A.* **2006**, *103*, 15315−15320.
(16) Gan, Y. D.; Dong, D. H.; Carlotti, S.; Hogen-Esch, T. E. *J. Am. Chem. Soc.* **2000**, *122*, 2130−2131.
(17) Nossarev, G. G.; Hogen-Esch, T. E. *Macromolecules* **2002**, *35*, 1604−1610.
(18) Chen, R.; Zhang, X.; Hogen-Esch, T. E. *Macromolecules* **2003**, *36*, 7477−7483.
(19) Hogen-Esch, T. E. *J. Polym. Sci., Part A: Polym. Chem.* **2006**, *44*, 2139−2155.
(20) Tezuka, Y.; Oike, H. *Prog. Polym. Sci.* **2002**, *27*, 1069−1122.
(21) Jia, Z. F.; Fu, Q.; Huang, J. L. *Macromolecules* **2006**, *39*, 5190−5193.
(22) Singla, S.; Zhao, T.; Beckham, H. W. *Macromolecules* **2003**, *36*, 6945−6948.
(23) Nakayama, Y.; Matsuda, T. *J. Polym. Sci., Part A: Polym. Chem.* **2005**, *43*, 3324−3336.
(24) Cramail, S.; Schappacher, M.; Deffieux, A. *Macromol. Chem. Phys.* **2000**, *201*, 2328−2335.
(25) Schappacher, M.; Deffieux, A. *Macromol. Chem. Phys.* **2002**, *203*, 2463−2469.

(26) Kubo, M.; Takeuchi, H.; Ohara, T.; Itoh, T.; Nagahata, R. *J. Polym. Sci., Part A: Polym. Chem.* **1999**, *37*, 2027−2033.
(27) Kubo, M.; Hibino, T.; Tamura, M.; Uno, T.; Itoh, T. *Macromolecules* **2002**, *35*, 5816−5820.
(28) Pantazis, D.; Schulz, D. N.; Hadjichristidis, N. *J. Polym. Sci., Part A: Polym. Chem.* **2002**, *40*, 1476−1483.
(29) Kolb, H. C.; Finn, M. G.; Sharpless, K. B. *Angew. Chem., Int. Ed.* **2001**, *40*, 2004−2021.
(30) Sharpless, K. B. *Angew. Chem., Int. Ed.* **2002**, *41*, 2024−2032.
(31) Tsarevsky, N. V.; Sumerlin, B. S.; Matyjaszewski, K. *Macromolecules* **2005**, *38*, 3558−3561.
(32) Laurent, B. A.; Grayson, S. M. *J. Am. Chem. Soc.* **2006**, *128*, 4238−4239.
(33) Kumar, R.; El-Sagheer, A.; Tumpane, J.; Lincoln, P.; Wilhelmsson, L. M.; Brown, T. *J. Am. Chem. Soc.* **2007**, *129*, 6859−6864.
(34) Xia, Y.; Yin, X.; Burke, N.; Stover, H. *Macromolecules* **2005**, *38*, 5937−5943.
(35) Xia, Y.; Burke, N.; Stover, H. *Macromolecules* **2006**, *39*, 2275−2283.
(36) Maury-Evertsz, J. R.; Lopez, G. E. *J. Chem. Phys.* **2005**, *123*, 054903.
(37) Qiu, X. P.; Tanaka, F.; Winnik, F. M. *Macromolecules* **2007**, ASAP Article, DOI: 10.1021/ma071359b, published on web 09/07/2007.
(38) Ciampolini, M.; Nardi, N. *Inorg. Chem.* **1966**, *5*, 41−44.
(39) Gao, H. F.; Matyjaszewski, K. *Macromolecules* **2006**, *39*, 4960−4965.
(40) Gao, H. F.; Matyjaszewski, K. *J. Am. Chem. Soc.* **2007**, *129*, 6633−6639.
(41) Whittaker, M. R.; Urbani, C. N.; Monteiro, M. J. *J. Am. Chem. Soc.* **2006**, *128*, 11360−11361.
(42) Teodorescu, M.; Matyjaszewski, K. *Macromolecules* **1999**, *32*, 4826−4831.
(43) Teodorescu, M.; Matyjaszewski, K. *Macromol. Rapid Commun.* **2000**, *21*, 190−194.
(44) Rademacher, J.; Baum, R.; Pallack, M.; Brittain, W.; Simonsick, W. *Macromolecules* **2000**, *33*, 284−288.
(45) Masci, G.; Giacomelli, L.; Crescenzi, V. *Macromol. Rapid Commun.* **2004**, *25*, 559−564.
(46) Flory, P. J. *Principles of Polymer Chemistry*; Cornell University Press: New York, 1953.
(47) Shan, J.; Chen, J.; Nuopponen, M.; Tenhu, H. *Langmuir* **2004**, *20*, 4671−4676.
(48) Kujawa, P.; Winnik, F. M. *Macromolecules* **2001**, *34*, 4130−4135.
(49) Tiktopulo, E. I.; Uversky, V. N.; Lushchik, V. B.; Klenin, S. I.; Bychkova, V. E.; Ptitsyn, O. B. *Macromolecules* **1995**, *28*, 7519−7524.

MA0717183